

Model for the A dependence of inclusive hadronic cross sections at large y and small \vec{p}_\perp

Bernice Durand and Jerome Krebs

Physics Department, University of Wisconsin, Madison, Wisconsin 53706

(Received 20 November 1979)

We present a new constituent-constituent multiple-scattering model for the A dependence of inclusive cross sections at large y and small \vec{p}_\perp , and we apply the model to $p + A \rightarrow \Lambda^0 + X$ data. We are able to extract from data the mean free path of the particles which interact with the nucleus A and a folding function which relates the cross sections for different A 's. The results confirm that the scattering is between constituents rather than between nucleons and suggest that the apparent number of constituents in the projectile at 300 GeV/c is about 5. The statistics are good enough to extract only two numbers, the mean free path of the constituents and the average change in rapidity per collision. We give the general shape of the scattering folding function. Data over a larger range of y would almost certainly reveal more structure in the folding function. We predict the $p + H \rightarrow \Lambda^0 + X$ cross section and suggest ways to analyze and display future data on A dependence.

I. BACKGROUND

Invariant inclusive hadronic cross sections from reactions in different nuclei (different atomic number A) are conventionally parametrized to display the A dependence as a single power α of A :

$$\frac{E d^3\sigma}{dp^3}(A, x, \vec{p}_\perp) = A^\alpha(\alpha, \vec{p}_\perp) E \frac{d^3\sigma}{dp^3}(1, x, \vec{p}_\perp). \quad (1)$$

The power α depends on x , the fraction of longitudinal momentum, and \vec{p}_\perp , the perpendicular momentum, of the measured particle, where the dependence on x and \vec{p}_\perp may also vary with A . Some data have been analyzed using a series in powers of $A^{1/3}$ to fit the cross section,

$$\frac{d\sigma}{dy} = A^{2/3}[\alpha(y) + A^{1/3}b(y) + A^{2/3}c(y)]. \quad (2)$$

In Eq. (2) the cross section is either at fixed \vec{p}_\perp or has been integrated over \vec{p}_\perp and is expressed in terms of the rapidity y instead of x .

In this paper we present a new constituent-constituent multiple-scattering model which gives a physical explanation of the features of Eq. (1) and leads to Eq. (2) as a series approximation.

One experiment which has been analyzed using both Eqs. (1) and (2) is $p + A \rightarrow \Lambda^0 + X$ by Heller *et al.*¹ In this experiment at 300 GeV/c the three targets used were Be, Cu, and Pb ($A=9, 64,$ and 208). The extrapolated $A=1$ cross section from Eq. (1) looks too large (see Fig. 1), while the $A=1$ cross section from Eq. (2) is close to the Be cross section (which seems more reasonable). When the Λ^0 data were being analyzed, L. Pondrom, one of the authors of Ref. 1, was interested in using Eq. (2) to fit the A dependence. One of us (B. D.) found at that time a multiple-scattering model which has Eq. (2) as an approximate solution. In this paper we give our current version of this

multiple-scattering model, together with applications of it to the Λ^0 data.

When this model was originally formulated, it was intended to describe constituent-constituent multiple scattering, not hadron-hadron multiple scattering. However, the basic equation, Eq. (3) (see below), would be valid for either constituent-constituent or hadron-hadron scattering and would yield Eq. (2) in either case. In fact, only by using the solution to Eq. (3) to fit data can one verify which particles are involved in the scattering. A

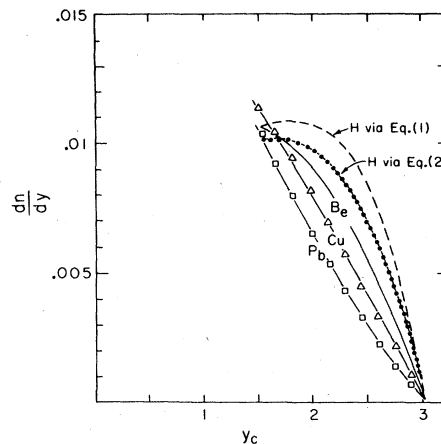


FIG. 1. The $p + A \rightarrow \Lambda^0 + X$ cross sections, integrated over \vec{p}_\perp and expressed in terms of $y_{c.m.}$ for $A=9$ (Be), 64 (Cu), 208 (Pb). The dashed curve is the prediction for $A=1$ (H) from Eq. (1) and the dotted curve is the prediction for $A=1$ from Eq. (2). This figure originally appeared in Ref. 1. The solid lines are the Be, Cu, and Pb data integrated over \vec{p}_\perp . The triangles and squares are predictions for the Cu and Pb distributions from Eq. (1.1). The quantity dn/dy from Ref. 1 corresponds to our $n(y)$. These curves were normalized to $\sigma_{\text{absorption } pp} = 46$ mb (an extrapolated value).

mean free path L appears in the model as a parameter. If the best fit to L had been $\sim 1.4 \times 10^{-13}$ cm, which is the mean free path of a proton in a nucleus, we would have concluded that the shift in the y distribution due to target size came from hadron-hadron scattering. We find from the Λ^0 data that L is $\sim 7.5 \times 10^{-13}$ cm. We conclude that there are between 5 and 6 constituents involved in the scattering process. The fits to $p + A \rightarrow \Lambda^0 + X$ in Ref. 1 using Eq. (2) were interpreted by the authors of that paper as resulting from hadron-hadron scattering. We hope that this present paper will convince the readers that the scattering is constituent-constituent, and we intend in the future to carry the model further to predict consequences due to different quark masses and different energy-loss processes.

Before presenting the model and results, we should point out that this multiple scattering is not of the Glauber² type. We regard all beam constituents as pointlike, not as being extended over enough space to simultaneously sample several target constituents. (It has recently been noted by Miettinen and Pumplin³ that the optical model is not reliable for A -dependence calculations.) Furthermore, we are not treating large- \vec{p}_\perp events, nor are we calculating constituent-hadron scattering, both of which are done in a recent article by Kryzwicki *et al.*⁴ The reader wishing to compare our model with others is referred to the new review of A dependence by Eilam *et al.*⁵ and references therein, and to the recent references listed collectively as Ref. 6.

One nice feature which emerged immediately from this model was that it is consistent with the long time scale built into Gottfried's⁷ explanation of slowly growing multiplicity. The final state need not coalesce until far downstream of the target; it will still exhibit the effects of constituent-

constituent scattering inside the target.

Another feature is that this model explains qualitatively the behavior of α in A^α of Eq. (1) as a function of x .⁸ In this model, any constituent can interact while traversing the nucleus (unlike the naive parton model). The interactions are not specified, but they include both soft interactions with radiation of energetic gluons and harder interactions which impart a fair amount of momentum to a target constituent. Thus all beam constituents lose momentum, including those at high x ; and the more matter traversed, the more momentum will be lost by the beam particles. However, the more matter traversed, the more possibilities there are for emitted gluons or target constituents to come out with low x . Thus a function of A high- x events are depleted while low- x events are augmented both by a beam shift from high to low x and by radiated or target particles gaining momentum. Parametrizing this by $A^{\alpha(x)}$ leads to α being smaller for high x than for low x .

Another feature is that the A dependence of any process involving the same constituents, including e^- , μ^- , γ^- , or ν -induced hadronic interactions, should be qualitatively the same. Various A targets thus become a laboratory for studying interactions of constituents.

II. THE MODEL

We assume that some initial number density n of constituents exists or is produced at $z=0$, where z is the beam direction and $z=0$ corresponds to the front surface of the target. The target is taken to be a disk of area $A^{2/3}$ and depth in the z direction proportional to $A^{1/3}$, as in Fig. 2. The number density n changes as the constituents travel through the nucleus according to the equation

$$dn(z, y, \vec{p}_\perp) = -\frac{dz}{L} n(z, y, \vec{p}_\perp) + \frac{dz}{L} \int_y^{y_{\max}} dy' \int_{-\infty}^{\infty} dp'_x \int_{-\infty}^{\infty} dp'_y F(y', y, \vec{p}'_\perp, \vec{p}_\perp) n(z, y', \vec{p}'_\perp). \quad (3)$$

The first term on the right side of Eq. (3) is a depletion term and the second is an augmentation term. L is the mean free path of a particle traversing the nucleus. The number density $n(y)$ is dN/dy , the number of particles with rapidity y in an interval dy . The invariant inclusive cross section $E d^3\sigma/dp^3 = \sigma_{\text{total}} dN/dy = \sigma_{\text{total}} n(y)$. (In Ref. 1 dN/dy is called dn/dy .) In our model σ_{total} is proportional to the area of the target. The limits on the y integral indicate that initially we have assumed that the particles only lose, never gain, y

in a collision.

The scattering equation can be easily solved if $F(y', y, \vec{p}'_\perp, \vec{p}_\perp)$ is a function of $y' - y$ and $(\vec{p}'_\perp - \vec{p}_\perp)^2$, and we assume for convenience that

$$F(y', y, \vec{p}'_\perp, \vec{p}_\perp) = f(y' - y) g((\vec{p}'_\perp - \vec{p}_\perp)^2). \quad (4)$$

We perform a Laplace transform on $(y' - y)$ and a Fourier transform on $(\vec{p}'_\perp - \vec{p}_\perp)$, calling the Laplace-transformed variable η and the Fourier-transformed variable \vec{q} ; we use tilde to denote Laplace transform and caret to denote Fourier

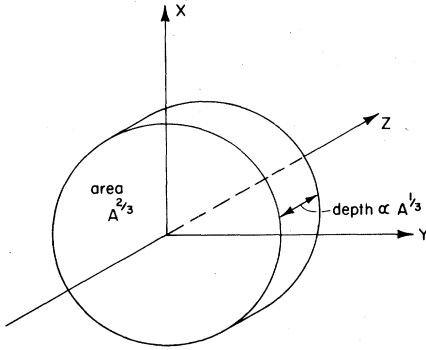


FIG. 2. The geometry of Eq. (3). We assume that the target nucleus is a disk of area $A^{2/3}$ and depth proportional to $A^{1/3}$. The beam direction is \hat{z} .

transform. The exact solution to the transformed equation is

$$\hat{n}(z, \eta, \vec{q}) = e^{-z/L} \exp[(z/L) \hat{f}(\eta) \hat{g}(\vec{q}^2)] \hat{n}(0, \eta, \vec{q}). \quad (5)$$

We should comment on a few points. In this simple model many questions are ignored in the interests of solving the equation and concentrating on a qualitative picture. For example, we cannot say where $z=0$ in $n(0, y, \vec{p}_\perp)$ should be. We should probably average over the nucleus to allow for the inelastic interaction which produces the stream of constituents to happen anywhere. Instead we take $n(0)$ as given at the surface of the target. Likewise, a disk is not necessarily the best geometry except mathematically. We might have taken a sphere and averaged z over path lengths, and in fact in Eq. (10) we will use a value of the proton mean free path for a spherical nucleus.

Initially, we believed that F , f , and g should all be normalized to 1. We changed our opinion on this when we found that a normalized f would not fit the Λ^0 data. Thus F really includes some excess (particle "production") from target constituents having their momentum boosted in collisions or fragmentation of beam particles, e.g., gluon emission. And thus the y integral limits are not really y and y_{\max} since some particles could reach y from below.

We have assumed separability as in Eq. (4) which would be in violation of energy-momentum conservation, since y is a function of p_\perp , but fortunately the data are expressed in terms of y_\parallel . Also, we argue below that the \vec{p}_\perp dependence is weak. Equation (3) has also been solved by iteration, yielding the same result as with transforms.

Neither f nor g is a known function. To get a physical picture of what is happening in \vec{p}_\perp , it is useful to assume that $\hat{g}(\vec{q}^2)$ has a maximum at $\vec{q}^2=0$:

$$\hat{g}(\vec{q}^2) \approx \hat{g}_0 - \frac{1}{2} \hat{g}_0'' \vec{q}^2. \quad (6)$$

The exponential part of Eq. (5) is now

$$\exp\left(\frac{z}{L} (\hat{f} \hat{g}_0 - 1)\right) \exp\left(-\frac{1}{2} \frac{z}{L} \hat{g}_0'' \vec{q}^2\right).$$

The inverse Fourier transform of this contains a Gaussian in $(\vec{p}'_\perp - \vec{p}_\perp) = \Delta \vec{p}_\perp$,

$$\exp\left(-\frac{\vec{q}^2}{2a^2}\right) \xrightarrow{\text{FT}^{-1}} \exp\left(-\frac{1}{2} \frac{\Delta \vec{p}_\perp^2}{b^2}\right). \quad (7)$$

This Gaussian dependence can be interpreted as the outcome of a random walk in \vec{p}_\perp , which is reasonable for a multiple-scattering model, especially for small \vec{p}_\perp .

Equation (5) can be written in three alternative ways:

$$\hat{n}(z, \eta, \vec{q}) = \hat{h}(z, \eta, \vec{q}^2) \hat{n}(0, \eta, \vec{q}), \quad (8a)$$

$$\hat{n}(z, \eta, \vec{q}) = e^{-z/L} \left[1 + \frac{z}{L} \hat{f} \hat{g} + \frac{1}{2!} \left(\frac{z}{L}\right)^2 (\hat{f} \hat{g})^2 + \dots \right] \times \hat{n}(0, \eta, \vec{q}), \quad (8b)$$

$$\hat{n}(z, \eta, \vec{q}) = \left[1 + \frac{z}{L} (\hat{f} \hat{g} - 1) + \frac{1}{2!} \left(\frac{z}{L}\right)^2 (\hat{f} \hat{g} - 1)^2 + \dots \right] \times \hat{n}(0, \eta, \vec{q}). \quad (8c)$$

We use the inverse transform of (8b) to fit data. In Ref. 1, a folding function which was essentially $h(z, y, \vec{p}_\perp^2)$ from the inverse transform of (8a) was used to fit the Be and Cu cross sections and predict the Pb and (unknown) H cross sections. Later in Ref. 1, the cross sections were fitted by Eq. (2), which was justified by comparison to our inverse transformed series (8c) truncated after the third term.

The inverse Laplace and Fourier-transformed Eq. (8b) is

$$n(z, y, \vec{p}_\perp) = e^{-z/L} \left[n(0, y, \vec{p}_\perp) + (z/L) fg * n(0, y, \vec{p}_\perp) + \frac{1}{2!} (z/L)^2 fg * fg * n(0, y, \vec{p}_\perp) + \dots \right], \quad (9)$$

where $*$ stands for convolution in y and \vec{p}_\perp .

The empirically obtained "best" folding function in \vec{p}_\perp from Ref. 1 is a sufficiently sharp Gaussian to be taken to be a δ function. This justifies dropping the g 's from Eq. (9). Using Eq. (9) with only the $f(y' - y)$ folding function, we have fitted data at fixed \vec{p}_\perp and data integrated over \vec{p}_\perp . (The integration of data was done by Heller *et al.*)

The average distance z traveled in nuclear matter is given by Hahn *et al.*⁹ as

$$z = A^{1/3} \times 1.5 \times 10^{-13} \text{ cm.}$$

Thus, depending on the mean free path L , k terms of the series in Eq. (9) must be used to fit cross sections until $(1/k!)(z/L)^k$ is sufficiently small.

We have found that we must keep the $(z/L)^2$ term to fit the Cu data and the $(z/L)^5$ term to fit the Pb data.

Our inverse-transformed series (8b), fixing \bar{p}_1 , becomes

$$n(A_2, y) = e^{-(z_2 - z_1)/L} \left[\delta_* + (A_2^{1/3} - A_1^{1/3}) \left(\frac{1.5 \times 10^{-13} \text{ cm}}{L} \right) f_* + \frac{1}{2} (A_2^{1/3} - A_1^{1/3})^2 \left(\frac{1.5 \times 10^{-13} \text{ cm}}{L} \right)^2 f_* f_{**} + \dots \right] n(A_1, y). \quad (10)$$

We used this formula to fit the Be, Cu, and Pb data and predict the H cross section.

III. FITS OF Λ^0 DATA

Before applying Eq. (10) to the Λ^0 data at $\bar{p}_1 = 0$ ("zero milliradian" data), we smoothed the Be data. We used this smoothed data for the $n(A_1, y)$ in Eq. (10). It was found when applying Eq. (10) to the Be data and fitting $n(A_2, y)$ to the Cu and Pb data separately, that no matter what folding function $f(y' - y)$ is used, the best value of L for the Cu data is the same as the best value of L for the Pb data, within a few percent. This is what is expected if L is independent of the nucleus in question because

$$\begin{aligned} z_2 - z_1 &\propto A_2^{1/3} - A_1^{1/3} \\ &= (4.0 - 2.1) \text{ for } A_2 = \text{Cu}, A_1 = \text{Be} \\ &= (5.9 - 2.1) \text{ for } A_2 = \text{Pb}, A_1 = \text{Be}, \end{aligned}$$

and 3.8 is twice 1.9. We believe that this independence of the mean free path is a strong feature of the model.

We considered different forms with free parameters for $f(y' - y)$. This gave us a set of folding functions which would predict the Cu and Pb data based upon the Be data. These folding functions were used in Eq. (10), with $n(A_1, y)$ the

smoothed Be data. The Cu and Pb data were fitted to $n(A_2, y)$ simultaneously. When doing these fits L and the parameters in the folding functions were varied. The results are given in Table I.

We note from Table I that L and Δy_{ave} are roughly independent of the shape of $f(y' - y)$. These seem to be the parameters that our model is most sensitive to. The significance of Δy_{ave} can be seen in Fig. 3 as the shift in the peak of the cross section from one A to another, although the range of y is too small to really check this for Cu and Pb.

The area under f is always greater than one, which means that the number of particles is not conserved. An explanation of this follows. A change in y of 0.7 corresponds to a reduction in p_z by a factor of 2. If the beam particle loses half its momentum in a scattering, the target particle which picked up that momentum or the fragment which carried off that momentum may appear in the final state. Thus we expect contributions from the target and fragments except for very high y . The area under our best f is 1.6 and the average change in y is 0.91, which corresponds to $p_z - 0.4p_z$. The value of Δy_{ave} was surprisingly high, indicating harder collisions than initially expected, although the peaks in Fig. 3 do bear out this shift.

We compare L with the mean free path of a proton in a nucleus,

TABLE I. The Cu and Pb data were simultaneously fitted to the smoothed Be data using the folding function $f(y)$. Polynomial f 's gave better fits than exponential f 's and the best $\chi^2/\text{d.f.}$ was for $f(y) = a + by$ with $a = 0.37$ and $b = 0.94$. Coupled with f is the value of the parameter L , which in fact is nearly independent of the form of f . L is the mean free path of a constituent and is 5.4 times the proton mean free path for our best $f(y)$. The average shift in y and the area under $f(y)$ are given. Area in excess of one is due to target constituents and beam fragmentation.

$f(y)$	Best parameters			L (cm)	L/L_p	Average Δy	Area under $f(y)$	$\chi^2/\text{d.f.}$
	a	b	c					
$f(y) = a$	0.8			7.0×10^{-13}	5.0	0.8	1.2	72/46 = 1.6
$f(y) = by$		1.8		8.0×10^{-13}	5.7	1.0	2.0	70/46 = 1.5
$f(y) = a + by$	0.37	0.94		7.5×10^{-13}	5.4	0.9	1.6	62/45 = 1.4
$f(y) = a + by + cy^2$	0.37	0.94	2×10^{-4}	7.5×10^{-13}	5.4	0.9	1.6	62/44 = 1.4

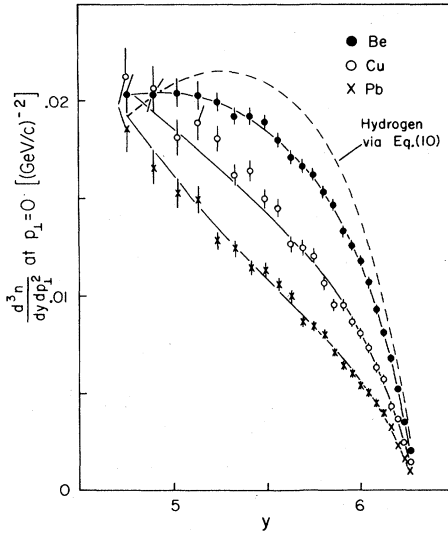


FIG. 3. The $p+A \rightarrow \Lambda^0 + X$ cross sections at $\vec{p}_{\perp 1} = 0$ and expressed in terms of y_{1ab} for Be, Cu, and Pb. The line through the Be data represents smoothed data. The lines through the Cu and Pb data are the best joint fit via Eq. (10), the solution to Eq. (3) for fixed $\vec{p}_{\perp 1}$. The dashed line is our predicted $A=1$ (H) cross section. These curves have been normalized to the total cross sections for $p+A$ for each A , which are proportional to $A^{2/3}$.

$$L_p = 1.4 \times 10^{-13} \text{ cm}$$

$$= \frac{1}{\sigma n},$$

where σ is the total absorption cross section of 40 mb and n is the nuclear density $[\frac{4}{3}\pi(1.1 \times 10^{-13} \text{ cm})^3]^{-1}$.

The connection between L_p and our L can be seen from the following naive argument, where p stands for proton (hadron), c for constituent, and N_c for the number of constituents per proton (hadron):

$$L_p = \frac{1}{\sigma_{pp} n_p},$$

$$L_c = \frac{1}{\sigma_{cc} n_c} = \frac{1}{\frac{1}{N_c} \sigma_{cp} N_c n_p}$$

$$= \frac{N_c}{\sigma_{pp} n_p} = N_c L_p.$$

Thus if our multiple scattering is between constituents, we would expect the mean free path L in Eq. (3) to be $L = L_c = N_c L_p$. From the Λ^0 data

we find $L \cong 5.4 L_p$. This confirms that it is the constituents which are interacting. It also indicates that there are 5 to 6 constituents in whatever went through the nucleus and later produced a Λ^0 .

In Table I, the fit $f(y) = 0.37 + 0.94y$ is the best fit to Cu and Pb data simultaneously, which gives a $\chi^2/\text{d.f.}$ of 1.4. When the Cu and Pb data were fitted separately to $f(y) = a + by$, we got $\chi^2/\text{d.f.} = 1.2$ for Cu and $\chi^2/\text{d.f.} = 1$ for Pb. When we fitted the data integrated over $\vec{p}_{\perp 1}$ by Heller *et al.* instead of the smaller number of data at fixed $\vec{p}_{\perp 1} = 0$, we found a folding function f with more structure than $a + by$. However, we had no errors on the integrated data and thus could not calculate a $\chi^2/\text{d.f.}$ We have, therefore, not presented that result.

In Fig. 3 we show the result of the $a + by$ fit to f from Table I and our prediction for the $p+H \rightarrow \Lambda^0 + X$ cross section. To get the H cross section from Eq. (10), we again let $n(A_1, y)$ be the smoothed Be data. The value of A_1 is then 9 and A_2 is 1.

We will now compare our analysis with that of Ref. 1. Our z is a continuous variable, so the series can be used for any value of A . Part of the analysis in Ref. 1 was done using discrete z , by noting that there is roughly one more nucleon mean free path in Cu than in Be, and in Pb than in Cu. Then each folding represents an extra collision between nucleons which would be equivalent to using the inverse-transformed (8a):

$$n(\text{Cu}) = h * n(\text{Be}),$$

$$n(\text{Pb}) = h * h * n(\text{Be}),$$

$$n(\text{Be}) = h * n(\text{H}).$$
(11)

Since \hat{h} is an exponential, $h(z) * h(z) = h(2z)$. The function h includes *all* powers of $A^{1/3}$. We note that $A^{1/3}$ for H, Be, Cu, Pb is 1, 2, 4, 6 approximately, so that the discrete folding for Be \rightarrow Cu \rightarrow Pb may be very good, but H would not be expected to be one mean free path shorter than Be. Thus our extrapolated H cross section comes from setting $A_2^{1/3} = 1$ in z_2 ; and in Ref. 1 the extrapolated hydrogen cross section comes from setting $A = 1$ in Eq. (2), which should give the same result as long as we keep only three terms in our series. Any difference between Figs. 1 and 3 is due to the $\vec{p}_{\perp 1}$ integration.

In Ref. 1 the three functions $a(y)$, $b(y)$, and $c(y)$ in Eq. (2) were fitted to the data from the three cross sections for Be, Cu, and Pb. Our Eq. (8c) has the form (omitting $\vec{p}_{\perp 1}$ and performing the inverse transform)

$$n(A, y) = \left[n(0, y) + A^{1/3} \left(\frac{1.5 \times 10^{-13} \text{ cm}}{L} \right) (f - \delta) * n(0, y) + \frac{1}{2} A^{2/3} \left(\frac{1.5 \times 10^{-13} \text{ cm}}{L} \right)^2 (f - \delta) * (f - \delta) * n(0, y) + \dots \right],$$
(12)

where $n(0, y)$ is obtained from the Be data and Eq. (10) with $A_2 = 0$. To convert $n(A, y)$ to a cross section $(d\sigma/dy)(A, y)$, we multiply by a constant times $A^{2/3}$ (the area of the target). $d\sigma/dy = (\text{const})A^{2/3}n(y)$. Assuming that n is approximately normalized, we define $A^{2/3}a(y) = \sigma_{\text{total}}n(0, y)$, and we get

$$\frac{d\sigma}{dy}(A, y) = A^{2/3} \left[a(y) + A^{1/3} \left(\frac{1.5 \times 10^{-13} \text{ cm}}{L} \right) (f - \delta) * a(y) + \frac{A^{2/3}}{2} \left(\frac{1.5 \times 10^{-13} \text{ cm}}{L} \right)^2 (f - \delta) * (f - \delta) * a(y) + \dots \right].$$

The first three terms in this series clearly resemble Eq. (2) if we make the identifications

$$b(y) = \left(\frac{1.5 \times 10^{-13} \text{ cm}}{L} \right) (f - \delta) * a(y),$$

$$c(y) = \frac{1}{2} \left(\frac{1.5 \times 10^{-13} \text{ cm}}{L} \right)^2 (f - \delta) * (f - \delta) * a(y).$$

We have found, however, that four or five terms should be kept for Pb or higher A targets. In fact, there will be (small) contributions from second and possibly higher-order terms even in cross sections for small A , such as H, depending on the magnitude of $(1.5 \times 10^{-13} \text{ cm})/L$. This analysis is pictured in Fig. 4. Figure 4 should be compared with Fig. 5, which is taken from Ref. 1. Note the different scales in Figs. 4 and 5. The different scales reflect the fact that the data in Ref. 1 were integrated over \vec{p}_1^2 while we used data at fixed $\vec{p}_1 = 0$. It is the shapes of $a(y)$, $b(y)$, and $c(y)$ which we wish to illustrate.

Since $a(y)$ is defined in terms of $n(0, y)$, we have found at least the shape of the initial y distribution. The area under $a(y)$ is related to a constituent cross section and the area under $a(y)$ multiplied

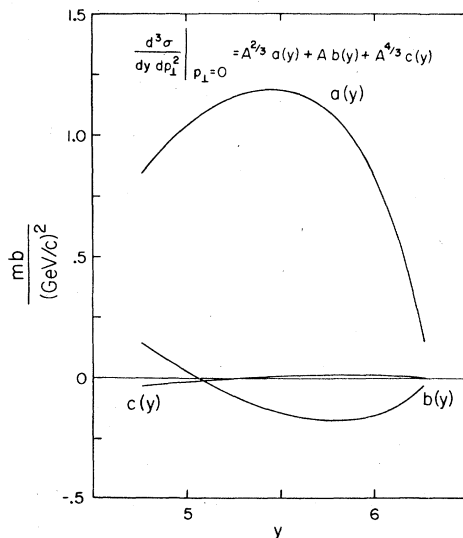


FIG. 4. The first three terms in the series of Eq. (10), corresponding to Eq. (2), plotted vs y_{lab} for $\vec{p}_1 = 0$. The vertical scale is $\text{mb}/(\text{GeV}/c)^2$.

by $A^{2/3}/\sigma_{\text{total}}$ is the number of constituents $\int dy n(0, y)$. We cannot say much more about constituent cross sections or numbers from Figs. 4 and 5 because we know $a(y)$ only over a very limited range of y and we do not know the overall normalization factor which would get us from σ_{total} for hadrons to σ_{total} for constituents.

Although $c(y)$ is very small on Fig. 4, $A^{4/3}$ can be quite large (~ 1200 for Pb). It is typical in experimental papers to use Eq. (2) with only three terms. Our $d(y)$ was too small to plot, but did contribute significantly to the Pb cross section. We thus recommend carrying the series as far as necessary. Since c, d, \dots all can be found from a and b , one is not restricted to three functions by having only three cross sections to fit.

IV. CONCLUSIONS

In conclusion, we suggest that data from different A targets be analyzed either at fixed \vec{p}_1 or integrated over \vec{p}_1 rather than at fixed angle. While the analysis could be carried out in terms of x , we have used y which has useful Lorentz properties. We further suggest that our Eqs. (10) and (12) be used to fit low- \vec{p}_1 data, keeping as many terms as necessary depending on z/L . It would

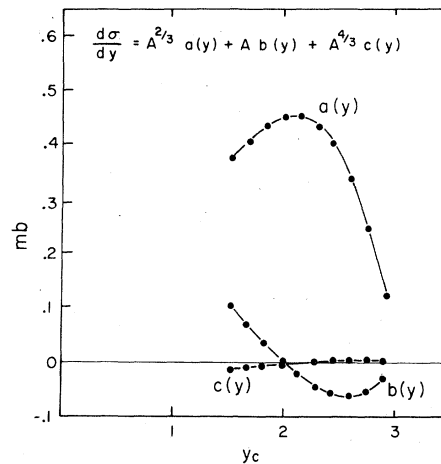


FIG. 5. The same three terms as ours in Fig. 4, from Ref. 1, plotted vs $y_{\text{c.m.}}$ for integrated \vec{p}_1 . The vertical scale is mb.

be interesting to compare the values of L and Δy_{ave} for other reactions to the values $L/L_p = 5.4$ and $\Delta y_{\text{ave}} = 0.91$ for $p + A \rightarrow \Lambda^0 + X$. We believe that the model can be refined to apply to all reactions by incorporating fragmentation functions, constituent structure functions, quark masses, careful consideration of energy-loss mechanisms, and retaining the \tilde{p}_1 dependence.

Our main result is that the A dependence of high- y , low- \tilde{p}_1 inclusive cross sections is well described by simple multiple scattering of the beam constituents from the target constituents. The model gives a power series in $A^{1/3}$ and explains the features of α in the customary A^α parametrization of A dependence. Each term in the power series represents one scattering. The physical picture is consistent with current ideas on the structure of hadrons and the interactions of quarks and

gluons. It suggests that A dependence can be used to investigate those interactions.

ACKNOWLEDGMENTS

We have both benefited from many conversations with L. Pondrom (whose data interested us in this problem) and with L. Durand. B. D. would like to thank the Aspen Center for Physics and the Theoretical Physics group at Caltech for hospitality while this work was in progress, and K. Gottfried, K. Lassila, G. Ringland, D. Snider, J. Vary, and G. Zweig for encouraging its publication. This research was supported in part by the University of Wisconsin Research Committee with funds granted by the Wisconsin Alumni Research Foundation, and in part by the U. S. Department of Energy under Contract No. DE AC02 76ER00881.

¹K. Heller *et al.*, Phys. Rev. D 16, 2737 (1977).

²R. J. Glauber, in *High Energy Physics and Nuclear Structure*, edited by G. Alexander (North-Holland, Amsterdam, 1967), p. 311.

³H. Miettinen and J. Pumplin, Phys. Rev. Lett. 42, 204 (1979).

⁴A. Krzywicki, J. Engels, B. Petersson, and U. Sukhatme, Bielfeld Report No. BI-TP 79/14, 1979 (unpublished).

⁵L. Bergström, G. Berlad, G. Eilam, and S. Fredriksson, Phys. Rep. (to be published).

⁶A. Białas and E. Białas, Phys. Rev. D 21, 675 (1980); A. Dar and F. Takagi, Phys. Rev. Lett. 44, 768

(1980); S. Hirabayashi *et al.*, Waseda Univ. Report No. KULA-HP-78-04 (unpublished); C. Michael and

D. Webber, Phys. Lett. 83B, 243 (1979); N. N. Nikolaev and S. Pokorski, Phys. Lett. 80B, 290 (1979).

⁷K. Gottfried, Phys. Rev. Lett. 32, 957 (1974).

⁸A fairly good parametrization of α for the Λ^0 data is $\alpha(x, \tilde{p}_1) = 0.4 + 0.48(1-x)^2 + 0.08\tilde{p}_1^2$. This fit has $\chi^2/\text{d.f.} = 41/24$. One of us (B.D.) suggested the form $\alpha = \alpha_0 + 0.5(1-x)^2 + 0.1\tilde{p}_1^2$ and Pondrom checked it while the data of Ref. 1 were being analyzed in 1977. However, Ref. 1 does not display $\alpha(x)$.

⁹B. Hahn, D. G. Ravenhall, and R. Hofstadter, Phys. Rev. 101, 1131 (1956).